SARS-CoV-2: what do we not know yet?

April, 21st, 2020

Barbara IIIi, PhD IBPM-CNR

Topics

- > CoV-2 structure
- >_Transcriptome and Interactome
- > Origin
- > Receptors
- > Variants
- > Clinical manifestations
- **≻Immunity**
- > Current therapies and preclinical vaccines

AIM

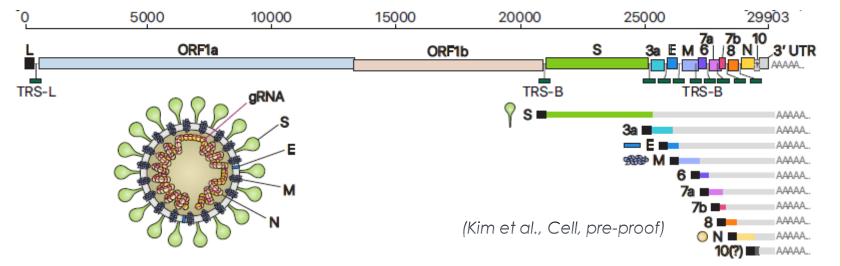
> Identification of possible approaches to answer unsolved questions



SARS-CoV-2 structure

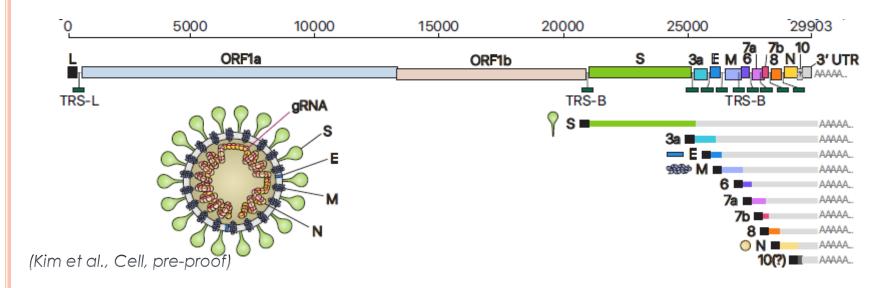
Coronaviridae family: positive-sense single-stranded RNA genome. Significant genetic variability and high recombination rate that enable them to be easily distributed among humans and animals worldwide.

Recently identified novel CoVs: SARS-CoV (2003); MERS-CoV (2012); nCoV-2019 (SARS-CoV-2; (2019).



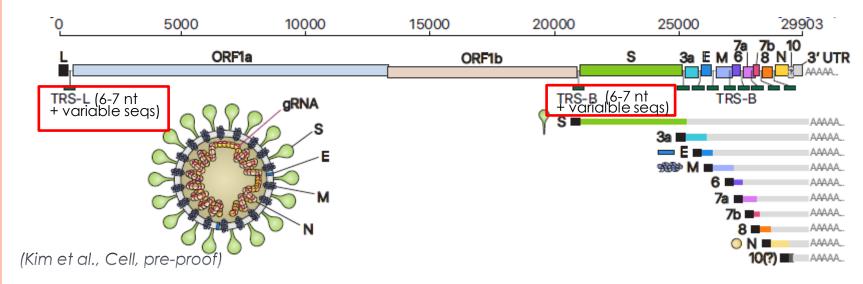
CoVs carry the largest genomes (26–32 kb) among all RNA virus families. Each viral transcript has a 5'-cap structure and a 3' poly(A) tail. Upon cell entry, the genomic RNA is translated to produce non structural proteins (nsps) from two open reading frames (ORFs), ORF1a, and ORF1b. The ORF1a produces polypeptide 1a (pp1a, 440–500 kDa). The –1 ribosome frameshift occurs immediately upstream of the ORF1a stop codon, which allows continued translation of ORF1b, yielding a large polypeptide (pp1ab, 740–810 kDa), which is cleaved into 16 nsps. The proteolytic cleavage is mediated by viral proteases nsp3 and nsp5 that harbor a papain-like protease domain and a 3C-like protease domain, respectively.

Replication and Transcription



Nsp12 harboring RNA-dependent RNA polymerase (RdRp) activity mediates replication and transcription. Negative-sense RNA intermediates are generated to serve as the templates for the synthesis of positive-sense genomic RNA (gRNA) and subgenomic RNAs (sgRNAs). The gRNA is packaged by the structural proteins to assemble progeny virions. Shorter sgRNAs encode conserved structural proteins (spike protein (S), envelope protein (E), membrane protein (M), and nucleocapsid protein (N)), and several accessory proteins. SARS-CoV-2 is known to have six accessory proteins (3a, 6, 7a, 7b, 8, and 10) according to the current annotation (GenBank: NC_045512.2). But the ORFs have not yet been experimentally verified for expression. It is currently unclear which accessory genes are actually expressed from this compact genome.

Replication and Transcription

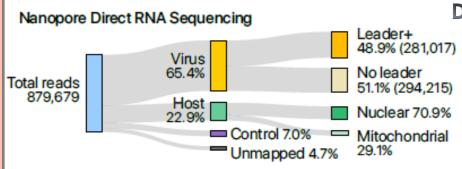


Each coronaviral RNA contains the common 5' "leader" sequence of ~70 nt fused to the "body" sequence from the downstream part of the genome. According to the prevailing model, leader-to-body fusion occurs during negative-strand synthesis at short motifs called transcription-regulatory sequences (TRSs, red boxes) that are located immediately adjacent to ORFs. TRS-L appears at 5' once in the viral genome. TRSs contain a conserved 6–7 nt core sequence (CS) surrounded by variable sequences. During negative-strand synthesis, RdRP pauses when it crosses a TRS in the body (TRS-B), and switches the template to the TRS in the leader (TRS-L), which results in discontinuous transcription leading to the leader-body fusion. From the fused negative-strand intermediates, positive-strand mRNAs are transcribed.

21/04/20

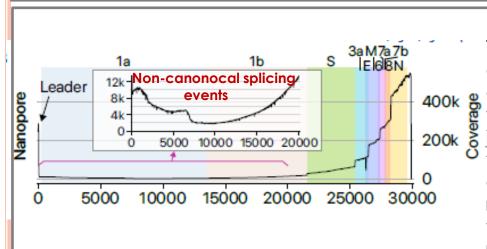
SARS-CoV-2 Transcriptome

- 2 complementary techniques: sequencing-by-synthesis (SBS by DNA nanoball sequencing) and nanopore-based direct RNA sequencing (DRS)
- Vero Cells infected with SARS-CoV-2
- > Throughput of 1.9 Gb



DRS runs on a MinION nanopore sequencer

The majority (65.4%) of the reads mapped to SARS-CoV-2, indicating that viral transcripts dominate the transcriptome while the host gene expression is strongly suppressed.

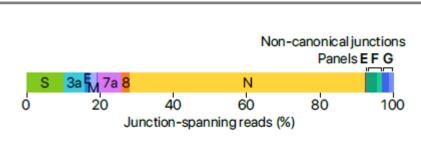


Genome coverage

The common presence of the leader sequence (72 nt) in viral RNAs results in a prominent coverage peak at the 5' end. Vertical drops in the coverage correspond to the leader-body junction in sgRNAs. Unexpected reads reflecting non-canonical "splicing" events were observed and were responsible for high coverage at 5' (inset). Some viral RNAs contain the 5' and 3' proximal sequences resulting from "illegitimate" polymerase jumping.

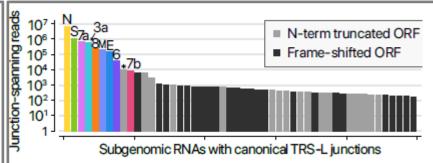
Data confirmed by DNA-nanoball sequencing (DNBSeq) (Kim et al., Cell, Apr 2020)

SARS-CoV-2 uses the canonical TRS-mediated template-switching mechanism for discontinuous transcription to produce major sgRNAs.

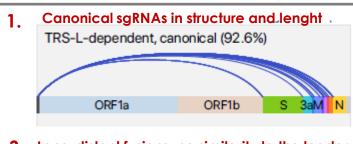


Transcript abundance estimated by counting the DNBseq reads that span the junction of the corresponding RNA

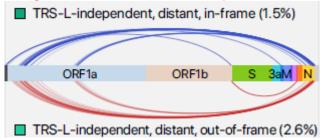
(Kim et al., Cell, Apr 2020)

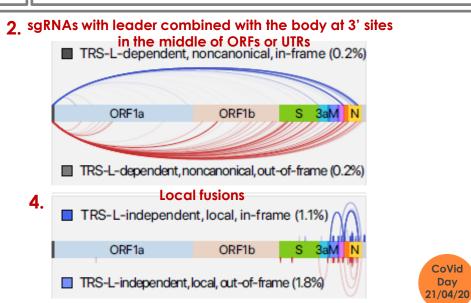


Top 50 sgRNAs. The asterisk indicates an ORF beginning at 27,825 which may encode the 7b protein with an N-terminal truncation of 23 amino acids. Grey and black bars denote minor transcripts.



3. Long-distant fusions, no similarity to the leader seq

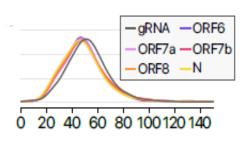


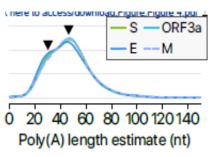


Some junctions show short sequences (3–4 nt) common between the 5' and 3' sites, suggesting a partial complementarity-guided template switching ("polymerase jumping"). But the majority do not have any obvious sequences. → Different transcription mechanisms? Non-canonical transcripts have a role in viral activity?

SARS-CoV-2 epitranscriptome

PolyA tail



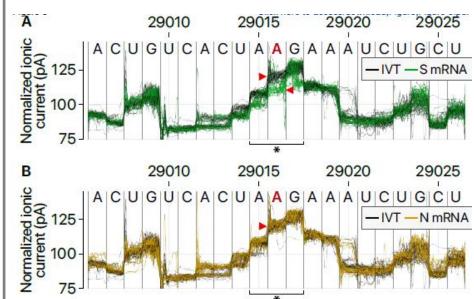


The tail of SARS-CoV-2 RNAs is 47 nt in median length. The full-length gRNA has a relatively longer tail than sgRNAs.

Notably, sgRNAs have two tail populations: a minor peak at ~30 nt and a major peak at ~45 nt (arrowheads). Bovine CoV mRNAs tail changes during infection: from ~45 nt immediately after virus entry to ~65 nt at

6–9 h.p.i. and \sim 30 nt at 120–144 h.p.i.. Thus, the short tails of \sim 30 nt observed in this study may represent aged RNAs that are prone to decay. Because poly(A) tail should be constantly attacked by host deadenylases, the regulation of viral RNA tailing is likely to be important for the maintenance of genome integrity. \rightarrow Is there any adenylyltransferase activity in Cov-2?

RNA modifications



Distinct ionic current signals ("squiggles") from viral S transcript (green lines) and in vitro transcribed control (IVT, black lines) indicate RNA modification at the genomic position 29,016. B, The ionic current signals from viral N transcript at the genomic position 29,016 (yellow lines) are similar to those from IVT control (black lines), indicating that modification is rare on the N sgRNA.

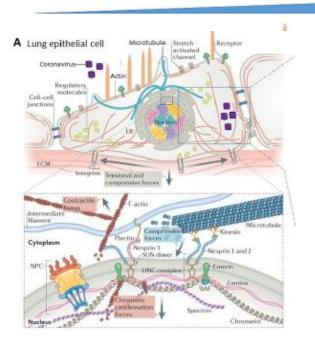
 \rightarrow No epi-modifications have been detected yet.

(Kim et al., Cell, Apr 2020)

21/04/20

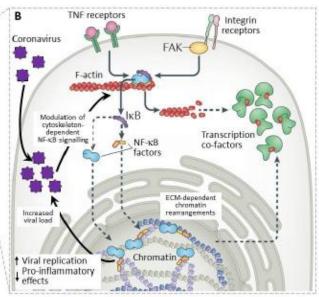
Perspectives on mechano-genomic regulation by SARS-CoV-2

hCoVs-induced transcripts in host cells include inflammatory genes and proteins activated by inflammatory signals, such as NF-kB. Importantly, NF-kB nuclear shuttling is regulated by actin depolimerization.



Changes of the extracellular matrix (ECM), including mechanical alterations such as stiffness, are transduced to the nucleus generally through the cytoskeleton networks of actin and microtubules as well as by regulatory molecules. These signals modulate the three-dimensional organization of chromosomes in the nucleus to regulate gene expression programs.

Ageing



Tissue Stiffness / Heterogeneity

Coronaviruses may take advantage of the cytoskeleton-dependent NF-kB signalling to the nucleus to upregulate genes that promote virus replication and propagation, while dampening the proinflammatory effects of this signalling. Such mechano-genomic regulation may be ageing-dependent. Depending on the age-increased lung tissue stiffness specific gene neighborhoods and transcription hotspots are formed in the genome, thus supporting the differential expression of various target genes including NF-kB targets (in this case skewing the target geneexpression towards virus-promoting signals)

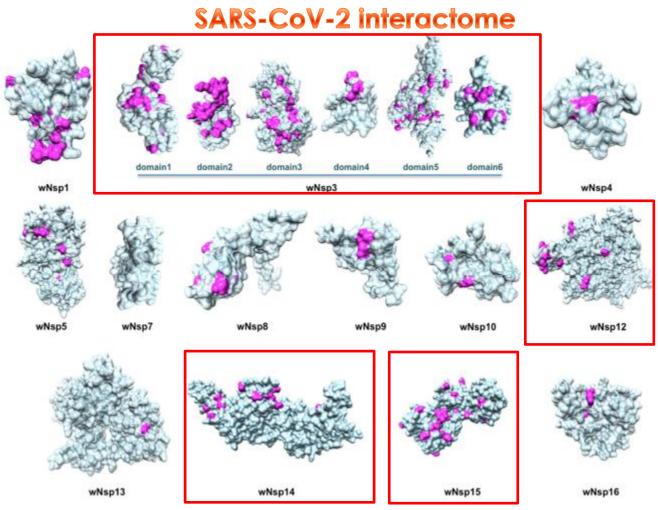
(Uhler and Shivashankar, Nat Rev Mol Cell Biol, Apr 2020)

SARS-CoV-2 interactome

The list of SARS-CoV-2 proteins analyzed and structurally characterized as in Srinvasan et al., Viruses, Feb 2020

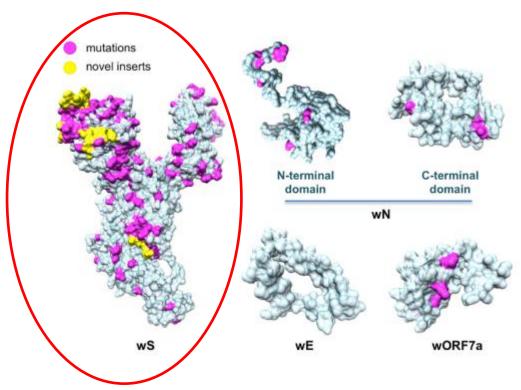
Protein	Accession	wORF1ab Region	Modeled Length	Template PDB id	Trgt-Tmplt Seq ID	Organism
wS, surface glycoprotein	YP_009724390		1273	6ACK	75%	SARS-CoV
wE, envelope protein	YP_009724392		75	5X29	89%	SARS-CoV
wORF7a	YP_009724395		121	1YO4	90%	SARS-CoV
wN, nucleocapsid phosphoprotein	YP_009724397		419	2JW8	96%	SARS-CoV
				1SSK	83%	SARS-CoV
				4UD1	51%	MERS-CoV
wNsp1	YP_009725297	13-127	115	2HSX	86%	SARS-CoV
wNsp3-domain1	YP_009725299	819-926	107	2GRI	79%	SARS-CoV
wNsp3-domain2	YP_009725299	1024-1198	175	2ACF	72%	SARS-CoV
wNsp3-domain3	YP_009725299	1232-1494	263	2WCT	76%	SARS-CoV
wNsp3-domain4	YP_009725299	1495-1550	66	2KAF	70%	SARS-CoV
wNsp3-domain5	YP_009725299	1564-1878	315	3E9S	82%	SARS-CoV
wNsp3-domain6	YP_009725299	1908-2763	113	2K87	82%	SARS-CoV
wNsp4	YP_009725300	3173-3263	91	3VC8	60%	MHV
wNsp5	YP_009725301	3264-3569	306	2GT7	96%	SARS-CoV
wNsp7	YP_009725302	3860-3942	83	1YSY	67%	SARS-CoV
wNsp8	YP_009725304	4019-4132	114	6NUR	85%	SARS-CoV
wNsp9	YP_009725305	4041-4253	113	3EE7	99%	SARS-CoV
wNsp10	YP_009725306	4262-4382	121	2G9T	98%	SARS-CoV
→ wNsp12	YP_009725307	4542-5311	770	6NUR	97%	SARS-CoV
wNsp13	YP_009725308	5325-5920	596	6JYT	100%	SARS-CoV
→ wNsp14	YP_009725309	5926-6451	526	5C8U	95%	SARS-CoV
→ wNsp15	YP_009725310	6452-6797	346	2H85	86%	SARS-CoV
wNsp16	YP_009725311	6800-7087	288	2XYQ	94%	SARS-CoV





Structurally characterized non-structural proteins of SARS-CoV-2. Highlighted in pink are mutations found when aligning the proteins against their homologs from the closest related coronaviruses: human SARS-CoV, bat coronavirus BtCoV, and another bat betacoronavirus BtRf-BetaCoV. The structurally resolved part of wNsp7 shares 100% sequence identity to its homolog. Mutated residues tended to locate on the protein's surface, supporting previous observations in other families of RNA viruses that the core residues of viral proteins were more conserved than the surface residues. In a substantial number of proteins, distributions of mutated positions exhibited spatial patterns, with groups of mutations found to form clusters on the protein surfaces. (*Srinvasan et al., Viruses, Feb 2020*)

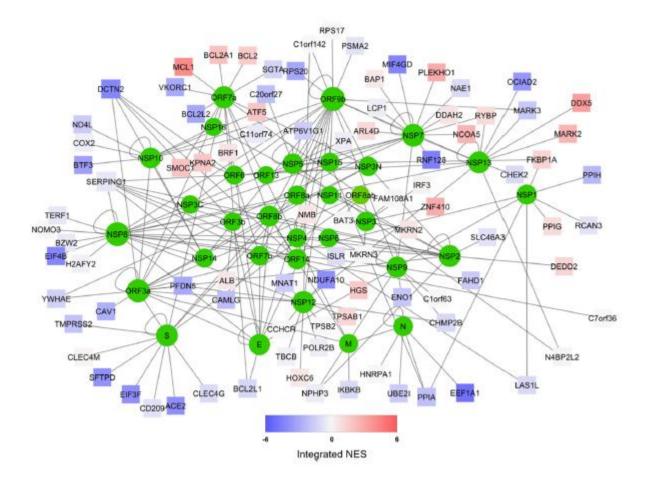
SARS-CoV-2 interactome



Structurally characterized structural proteins and an ORF of SARS-CoV-2. Highlighted in pink are mutations found when aligning the proteins against their homologs from the closest related coronaviruses: human SARS-CoV, bat coronavirus BtCoV, and another bat betacoronavirus BtRf-BetaCoV. Highlighted in yellow are novel protein inserts found in wS. (Srinvasan et al., Viruses, Feb 2020)

Day 21/04/20

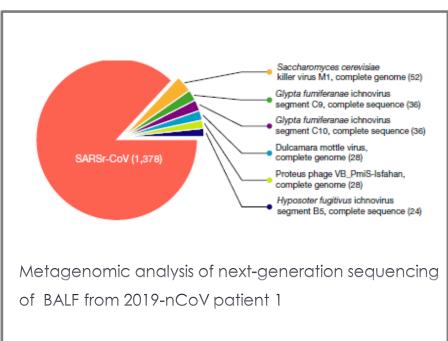
SARS-CoV-2 interactome

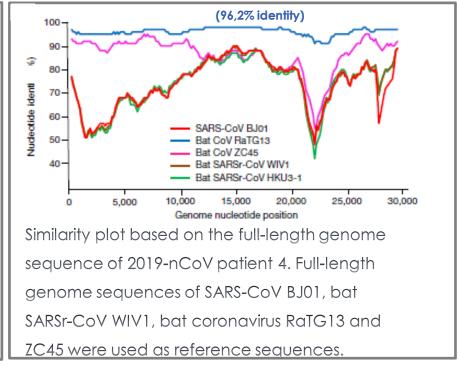


Representation of the predicted SARS-CoV-2/Human interactome, containing 200 unique interactions among 125 proteins (nodes). SARS-CoV-2 proteins are depicted as green circles, while human proteins are represented as squares. The color of human protein nodes reflects the integrated effect of MERS and SARS infections on the node network as a Normalized Enrichment Score (NES). (Guzzi et al., J Clin Med, Apr 2020)

SARS-CoV-2 origin: bat or pangolin?

CoV-2: Full-length genome sequences obtained from five patients at an early stage of the outbreak were almost identical (99.9%) and shared 79.6% sequence identity to SARS-CoV. Furthermore, 2019-nCoV is 96% identical at the whole-genome level to a bat coronavirus.





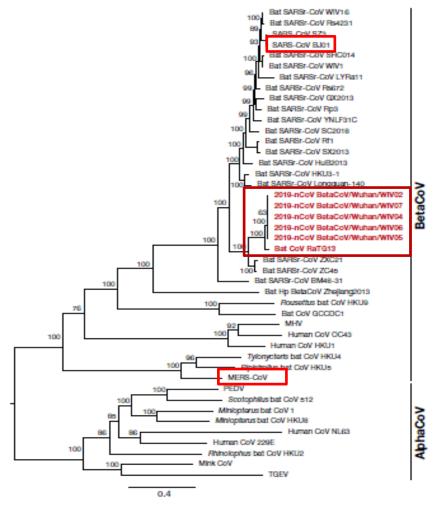
(Zhou et al., Nature, Feb 2020)



SARS-CoV-2 origin: bat or pangolin?

SARS-CoV and SARS-CoV-2 shred less than 80% sequence nucleotide identity. However, the amino acid sequences of the seven conserved replicase domains in ORF1ab were 94.4% identical between 2019-nCoV and SARS-CoV, suggesting that the two viruses belong to the same species, SARSr-

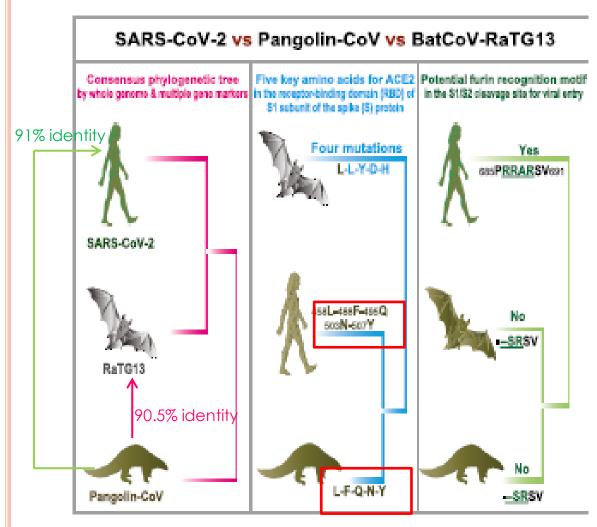
CoV.



Nevertheless, phylogenetic analysis of the full-length genome and the gene sequences of RdRp and spike (S) showed that—for all sequences—*RaTG13* is the closest relative of 2019-nCoV and they form a distinct lineage from other SARSr-CoVs.



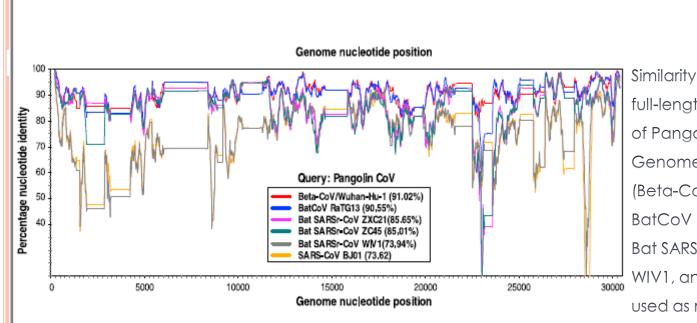
SARS-CoV-2 origin: bat or pangolin?



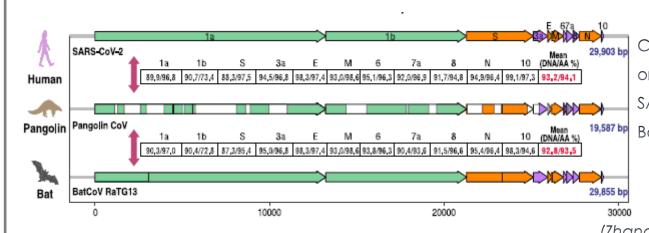
On 24 October 2019, the existence of a SARS-CoV-like CoV from lung samples of two dead Malayan pangolins with a frothy liquid in their lungs and pulmonary fibrosis was detected, close to when the COVID-19 outbreak occurred. All virus contigs assembled from two lung samples exhibited low identities, ranging from 80.24% to 88.93%, with known SARSr-CoVs. Hence, the dead Malayan pangolins likely carried a new CoV closely related to SARS-CoV-2 CoVid

Day 21/04/20

Pangolin as the common origin of BatCoVRaTG13 and human SARS-CoV-2



Similarity plot based on the full-length genome sequence of Pangolin-CoV. Full-length
Genome sequences of SARS-CoV-2
(Beta-CoV/Wuhan-Hu-1),
BatCoV RaTG13, bat SARSr-CoV 21,
Bat SARSr-CoV45, bat SARSr-CoV
WIV1, and SARSCoVBJ01 were used as reference sequences.

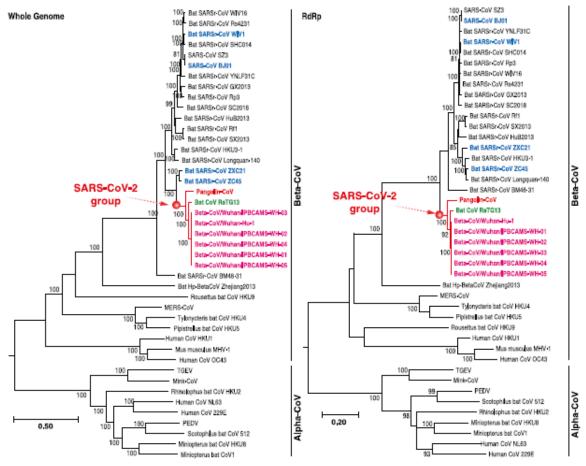


Comparison of common genome organization similarity among SARS-CoV-2, Pangolin-CoV, and BatCoV RaTG13.



(Zhang et al., Current Biol, Apr 2020)

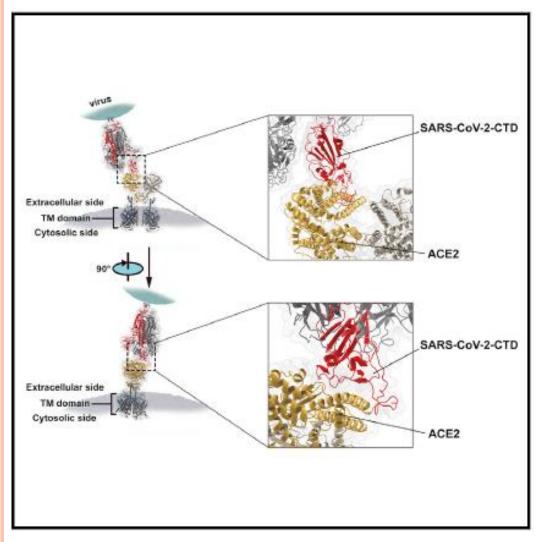
Pangolin-CoV is the common ancestor of BatCoVRaTG13 and human SARS-CoV-2



Phylogenetic Relationship of CoVs Based on the Whole Genome and RdRp Gene Nucleotide Sequences.

Furthermore: S1 protein of Pangolin-CoV is more closely related to that of SARS-CoV-2 than to that of RaTG13. Within the RBD, Pangolin-CoV and SARS-CoV-2 were highly conserved, with only one amino acid change (500H/500Q), which is not one of the key residues inolved in receptor binding. Therefore, Pangolin-CoV could have pathogenic potential similar to that of SARS-CoV-2.

SARS-CoV-2 infection

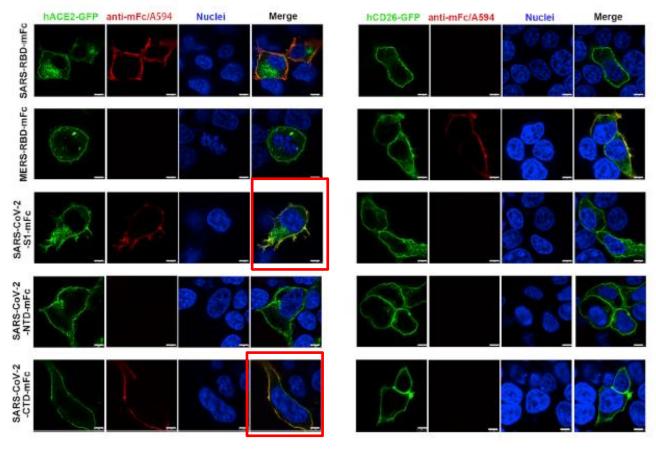


- >SARS-CoV-2 interacts with hACE2 via S protein CTD
- > A 2.5-Å structure of SARS-CoV-2-CTD in complex with hACE2 is resolved
- > The SARS-CoV-2-CTD displays stronger affinity for hACE2 compared with SARS-RBD
- > SARS-CoV-2 -CTD is antigenically different from SARS-RBD
- ➤The increased atomic interactions
 between the hACE2 and SARS-CoV-2CTD binding region leads to ~4-fold higher binding affinity compared with the
 SARS-RBD.

(Wang et al., Cell, May 2020)

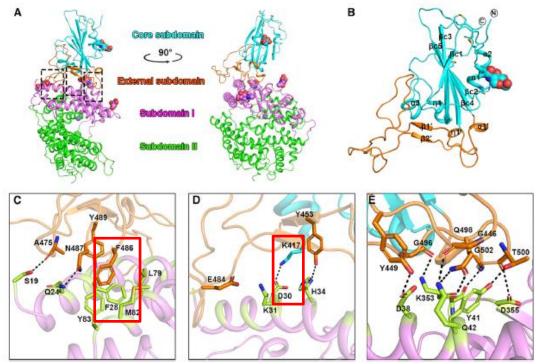


SARS-CoV-2 infection: SARS-CoV-2-S1 and SARS-CoV-2-CTD Colocalize with hACE2



HEK293T cells were transfected with pEGFP-N1-hACE2 (left panels, hACE2-GFP) or pEGFP-C1-hCD26 (right panels, hCD26-GFP). Twenty-four hours later, the cells were incubated with supernatant containing mFc-tagged SARS-CoV-2-S1 (SARS-CoV-2-S1-mFc), SARS-CoV-2-NTD (SARS-CoV-2-NTD-mFc), SARSCoV-2-CTD (SARS-CoV-2-CTD-mFc), MERS-RBD (MERS-RBD-mFc), or SARS-RBD (SARS-RBD-mFc) proteins and subsequently incubated with anti-mouse IgG (mIgG) antibody conjugated with A594 (anti-mIgG/A594). Nuclei were stained with DAPI. The scale bar in each panel indicates 8 μm (Wang et al., Cell, May 2020)

SARS-CoV-2 infection: crystal structure (2.5 Å) of CoV-2 CTD and hACE2 receptor



(Wang et al., Cell, May 2020)

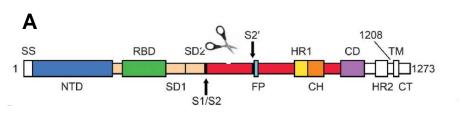
(A) A cartoon representation of the complex structure. The core subdomain and external subdomain in SARS-CoV-2-CTD are colored cyan and orange, respectively. hACE2 subdomain I and II are colored violet and green, respectively. The right panel was obtained by anticlockwise rotation of the left panel along a longitudinal axis. The contacting sites are further delineated in (C)–(E). for the amino acid interaction details. (B) A carton representation of the SARS-CoV-2-CTD structure.

The secondary structural elements are labeled according to their occurrence in sequence and location in the subdomains. Specifically, the b strands constituting the core subdomain are labeled with an extra c, whereas the elements in the external subdomain are labeled with an extra prime symbol. The disulfide bonds and N-glycan linked to N343 are shown as sticks and spheres, respectively. (C–E) Key contact sites are marked with the left, middle and right box in (A) and further delineated for interaction details, respectively. The residues involved are shown and labeled. Changes of L472 in SARS-CoV to F486 in CoV-2 may make stronger van der Waals interaction With M82 of hACE2- The substitution of V404 in SARS-CoV with K417 in CoV-2 may result in stronger association because of salt bridge formation between K417 of CoV-1 and D30 of

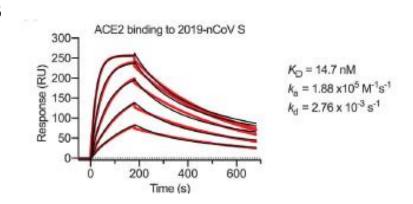
(Wang et al., Cell, May 2020)

hACE2.

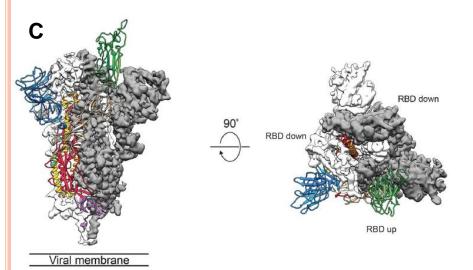
SARS-CoV-2 cell entry



A) The spike (S) protein of SARS-CoV-2 facilitates viral entry into target cells. Entry depends on binding of the surface unit, S1, of the S protein to a cellular receptor, which facilitates viral attachment



to the surface of target cells. In addition, entry requires S protein priming by cellular proteases, which entails S protein cleavage at the \$1/\$2 and the \$2' site and allows fusion of viral and cellular membranes, a process driven by the \$2 subunit. B) SARS-S engages angiotensin-converting enzyme 2 (ACE2) SPR shows the binding kinectics of ACE2 and immobilized CoV-2

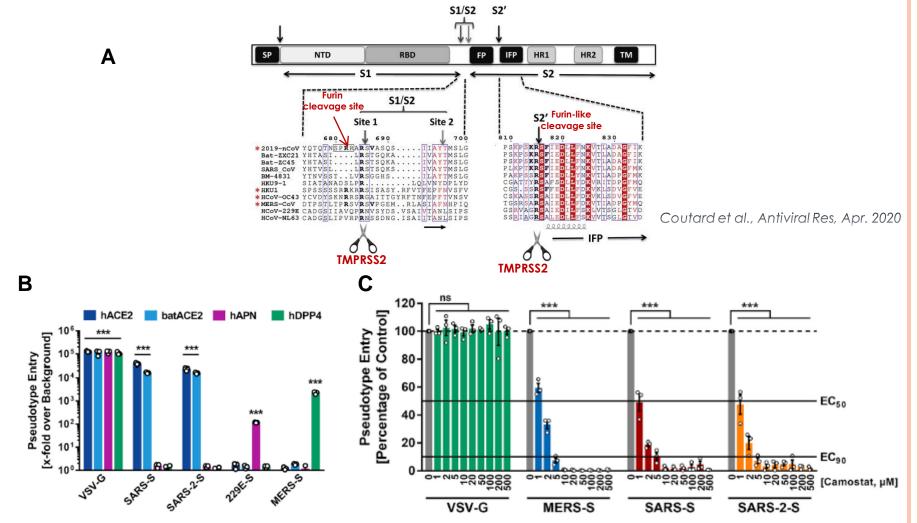


To engage a host cell receptor, the receptor-binding domain (RBD) of \$1 undergoes hinge-like conformational movements that transiently hide or expose the determinants of receptor binding. These two states are referred to as the "down"conformation and the "up" conformation, where down corresponds to the receptor-lnaccessible state and up corresponds to the receptor accessible state, which is thought to be less stable.

CoVid

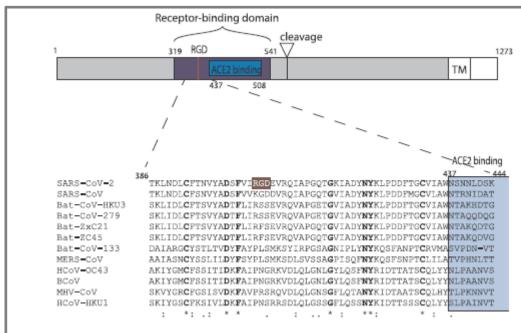
C) Side and top views of the prefusion cryoEM structure of the 2019-nCoV S protein with a single RBD in the up conformation, at 3.5 Å of resolution. The two RBD down protomers are shown as cryo-EM density in either white or gray and the RBD up protomer is shown in ribbons colored corresponding to the schematic in (A). (Wrapp et al., Science, Mar 2020)

SARS-CoV-2 cell entry requires TMPRSS2 protease

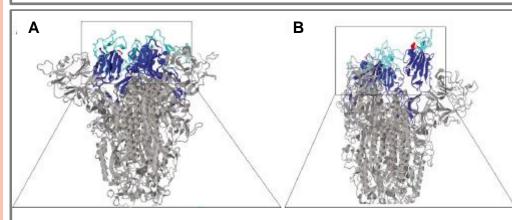


- A) Sequence similarity between SARS-CoV and SARS-CoV-2 S1/S2 and S2' domains. TMPRSS2 cleavage sites are indicated. B) Viral entry in BHK-21 cells transfected with human and bat receptors. C) TMPRSS2 inhibitor Camostat inhibits viral entry of cornovirus with different efficiency.(Hoffmann et al., Cell, Apr. 2020)
 - Single cell RNAseqs have revealed expression overlap of ACE2/TMPRSS2/Furin in human bronchial cells (Lukassen et al., EMBO J, Apr 2020)

SARS-CoV-2 cell entry: role of integrins?



Schematic representation of SARS-CoV-2 S-protein with a focus on the receptor-binding domain. The sequences of 12 betacoronavirus were aligned using MAFFT. The receptor-binding domain and the ACE2 receptor-binding region are colored in blue and light blue, respectively. The RGD motif of SARS-CoV-2 is highlighted in color.

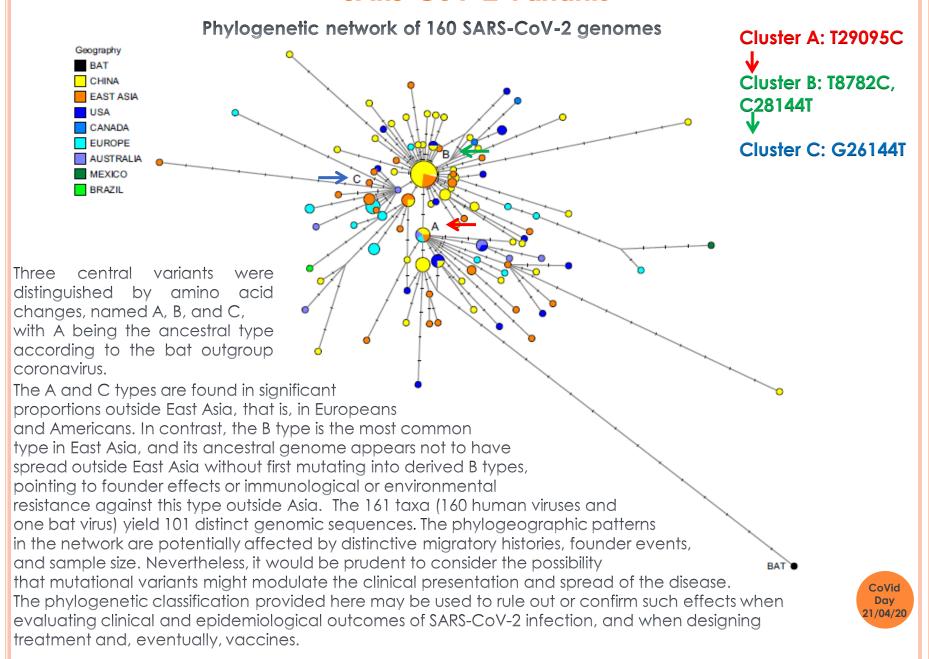


Model of SARS-CoV-2 structure provided by SWISSMODEL and visualized with Jmol.

A) The mushroom-like fold of the model is the classical one in absence of ligand binding. Ligand binding causes a drastic conformational change leading to the protrusion of one of the trimeric binding domains, further exposing the RGD-loop. The receptor-Binding domain is colored in blue, with a focus in light blue on the part

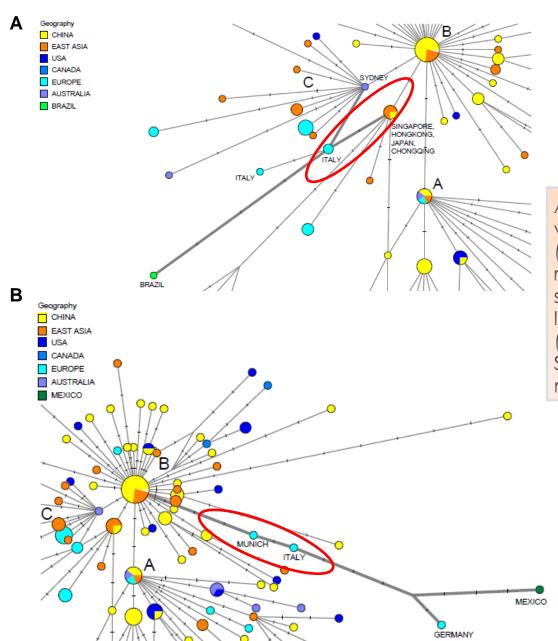
binding the receptor ACE2 The RGD motif is colored in red. B) Model of SARSCoV- 2 structure in the conformational state of ACE2-binding provided by SWISSMODEL and visualized with Jmol. The receptor-binding domain of the trimer is in the "up" conformation exposing the RGD motif. Same colors as in A. (Signist et al., Antiviral Res, Feb 2020)

SARS-CoV-2 Variants



(Forster et al., PNAS, Mar 2020)

SARS-CoV-2 Variants: Italy



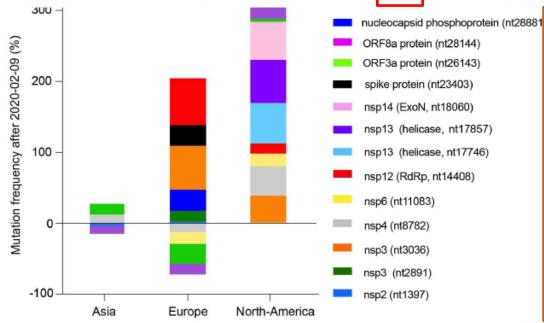
Apparently, in Italy we had two virus entries. One from East Asia (referred as the "Singapore variant", located in philogenetic cluster C (A) and one from Munich, located in philogenetic cluster B (B). Both genomes are linked to Singapore or Munich virus by 1 mutation difference.



SARS-CoV-2 RNA-dependent-RNA polymerase variant

(Pachetti et a., J Transl Med, Apr 2020)

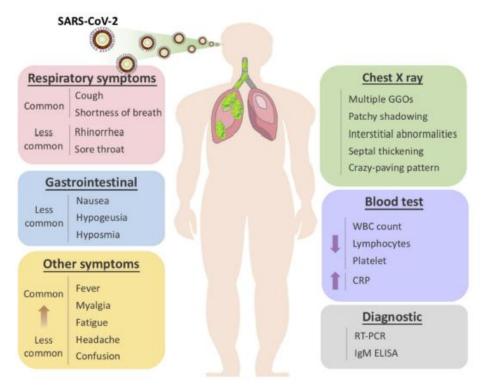
	n pts before	n pts after	1397	2891	3036	8782	11083	14408	17746	17857	18060	23403	26143	28144	28881
Europe	17	81	+2.5%	+14.8%	+61.7%	-12.7%	-22.9%	+60.5%	0%	0%	0%	48.1%	-46.5%	-15.2%	29.6%
Asia	59	12	-3.4%	0%	0%	11.3%	-0.14%	0%	0%	0%	0%	0%	+26.6.%	-15.2%	0%
North America	0	28	0%	0%	+35.7%	+42.9%	+17.9%	+14.3%	+57.2%	+60.7%	+53.4%	0%	+3.6%	+21.4%	+3.6%



The first appearance of RdRp mutation is manifested on February 9th, 2020 in the UK (England), when a dramatic increase of the number of European infected patients was reported from the WHO website In particular, a strong increase (+ 60.5%) of genomes carrying the 14408 mutation (affecting RdRp) was observed in Europe, together with an increase of genomes carrying the 3036 mutation (+ 61.7%), and the 28881 mutation (+29.6%)

- ➤ Homology between RdRps of SARS-CoV and SARS-CoV-2 indicates the amino acid substitution 323 (P to L) (due to nucleotide mutation 14408) falls outside the catalytic site in a region supposedly implicated in the interaction with other proteins which may regulate the activity of RdRp.
- SARS-CoV replication supercomplex interacts with nsp14, an exonuclease having the Nidovirales-typical proofreading capability. This activity is important in the context of the mutation rate and for controlling the fidelity in RNA replication. However, critical RdRp residues involved in this interaction are still to be identified, and for this reason further studies are needed to assess the possible role of mutation 14408 concerning RdRp fidelity.

CoVid-19



Clinical manifestations and diagnostic of CoVid-19

The U.S. Food and Drug Administration (FDA) has approved a SARS-CoV-2 commercial test system from Roche (cobas® SARS-CoV-2). This qualitative test requires samples from nasopharyngeal or oropharyngeal swabs, and it takes 3.5 hrs to yield the results. Based on RT-PCR methodology, the cobas SARS-CoV-2 test is a dual target assay, detecting both the specific SARS-CoV-2 RNA, as well as the highly conserved fragment of the E gene invariant in all members of the Sarbecovirus subgenus. The assay has a full-process negative control, positive control and internal control to ensure specificity and accuracy. On 21 March 2020, FDA granted another Emergency Use Authorization to Xpert® Xpress SARS-CoV-2 from Cepheid Inc (USA), which is also a qualitative test that claimed to yield the results within 45 min. (Tu et al., Int J Mol Sci, Apr 2020)

CoVid-19

Comparison among SARS-MERS- and SARS-CoV-2.

	SARS-CoV	MERS-CoV	SARS-CoV-2		
Disease	SARS	MERS	COVID-19		
Transmission	 Respiratory droplets Close contact with diseased patients Fecal-oral Aerosol [26] 	 Respiratory droplets Close contact with diseased patients/camels Ingestion of camel milk 	Respiratory droplets Close contact with diseased patients Possibly fecal-oral [7] Possibly aerosol [27]		
Latency	2–7 days	2–14 days	97.5% became symptomatic within 11.5 days (CI, 8.2 to 15.6 days) [28]		
Contagious period	10 days after onset of disease	When virus could be isolated from infected patients	Unknown		
Reservoir	Bats	Bats	Bats		
Incidental host	Masked palm civets	Dromedary camels	Malayan pangolin [29]		
Origin	Guangdong, China	Saudi Arabia	Hubei, China		
Fatality rate	~10%	~36%	~2.3%		
Radiologic features		tchy ground-glass opacities to bi adiograph. Non-specific to distir diseases. [30–33]			
Clinical presentation	failure leadir	l disease to acute upper respirato ng to death. Varies between indi iting and diarrhea are also repor	viduals. [34] Cardiovas		

A recent study suggested that the half-lives of SARS-CoV-2 and SARS-CoV were similar in aerosols with the median infectious period estimated to be around 1.1 to 1.2 hour. Therefore, as an echo to SARS-CoV, the possibility of air-borne and fecal-oral transmission of SARS-CoV-2 cannot be ruled out, however, more evidence is still needed. (Tu et al., Int J Mol Sci, Apr 2020)



CoVid-19Affects Women Less Than Men

- > Different innate immunity, steroid hormones and factors related to sex chromosomes
- The immune regulatory genes encoded by X chromosome in female gender causes lower viral load levels, and less inflammation than in man, while CD4+ T cells are higher with better immune response
- > Higher levels of antibodies which remain in the circulation longer.
- > The levels of activation of the immune cells are higher, and it is correlated with the trigger of TLR7 and the production of IFN
- > TLR7 biallelic expression leads to higher immune responses and increases the resistance to viral infections. TLR7 is expressed in innate immune cells which recognizes single strand RNA virus by promoting the production of antibodies against the virus and the generation of pro-inflammatory cytokines including IL-6 and IL-1 family members.
- > The production of inflammatory IL-6 after viral infection is lower
- > On the X chromosome there are loci that code for the genes involved in the regulation of immune cells such as FOXP3, and transcription factor for Treg involved in virus pathogenesis
- The X chromosome influences the immune system by acting on many other proteins, including TLR8, CD40L and CXCR3 which can be over-expressed in women, and influence the response to viral infections and vaccinations
- > TMPRSS2 is upregulated by androgens and deregulated in prostate cancer (Conti et al., J Biol Regul Homeost Agents, Apr 2020; Stopsack et al., Cancer Discov, Apr 2020)

SARS-CoV-2 Immunity: antibodies

Table 2. Performance of different detections in samples at different time since onset of patients.

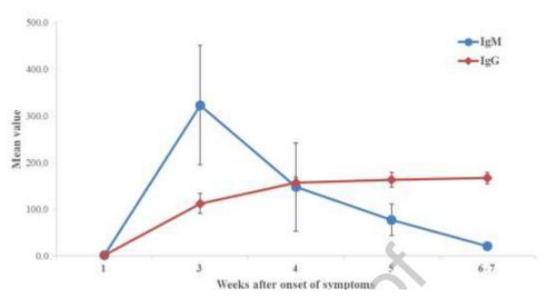
Days			RNA	•	Ab	•	lgM		lgG		RNA+Ab
after onset	n	n(+)	Sensitivity	n(+)	Sensitivity	n(+)	Sensitivity	n(+)	Sensitivity	n(+)	Sensitivity
			(%, 95%CI)		(%, 95%CI)		(%, 95%CI)		(%, 95%CI)		(%, 95%CI)
Total	472	112 ^{\$}	67.1	464	93.1	142	82.7	442	64.7	172	99.4
Total	173	112	(59.4, 74.1)		143	(76.2, 88)	112	(57.1, 71.8)	1/2	(96.8, 100.0)	
1-7	94	58 ^{\$}	66.7	36	38.3	27	28.7	18	19.1	74	78.7
1-7	34	30	(55.7, 76.4)	30	(28.5, 48.9)	21	(19.9, 39.0)	10	(11.8, 28.6)	14	(69.1, 86.5)
8-14	135	67 ^{\$}	54.0	121	89.6	99	73.3	73	54.1	131	97.0
0.14	100		(44.8, 63.0)	121	(83.2, 94.2)	00	(65.0, 80.6)	10	(45.3, 62.7)	101	(92.6, 99.2)
15-39	90	25 ^{\$}	45.5	90	100.0	83*	94.3	71#	79.8	90	100.0
			(32.0, 59.5)		(96.0, 100.0)		(87.2, 98.1)		(69.9, 87.6)		(96.0, 100.0)

Seroconversion rate for IgM and IgG from 173 CoVid-19 patients. The seroconversion time of IgM and IgG antibodies appeared consequently (p<0.05) with a median seroconversion day of 12 and 14, respectively. Notably, even in the early stages of the illness within 1-week, some patients with undetectable RNA could be screened out through Ab testing. Combining RNA and antibody tests significantly raised the sensitivity for detecting patients (p<0.001). These findings indicate that serological test be an important supplement to RNA detection during the illness course. In addition to the diagnosis value, a strong positive correlation between clinical severity and Ab titer since 2-week after illness onset was revealed, for the first time in COVID-19 patients. These results suggested that a high Ab titer may be considered as a risk factor of critical illness, independently from older age, male gender and comorbidities . (Zhao et al., Clin Infect Dis, Mar 2020)

Day 21/04/20

SARS-CoV-2 Immunity: antibodies

Figure 1. Timeline of IgM and IgG Antibodies level to SARS-CoV-2 from the Onset of Symptoms



In week 3 after symptoms onset, all patients (34) were tested positive for IgM and IgG. In week 4, all the results were still positive for IgM and IgG. IgM declined while IgG continued to go up. In week 5, however, all patients were positive for IgG, while 2 patients (16.7%) got negative results for IgM. IgM level kept going down and IgG continued to raise At the end of observation (7 weeks), 2 patients (33.3%) got negative results for IgM, while all patients positive for IgG. For SARS-CoV, studies revealed that IgM reached the highest point within 4 weeks and was not detectable on 3 months after onset of symptoms. IgG were persistently detectable up to 24 months. The profile of specific antibodies to SARS-CoV-2 seems to be similar to SARS-CoV. Detectable and continuous high level of IgM indicated the acute phase of infection. CoVid Furthermore, IgM last more than a month indicating the prolonged virus replication in Dav 21/04/20 SARS-CoV-2 infected patients, IgG responded later than IgM and persisted high in this study, Indicating the humoral immune reaction to protect the body against SARS-CoV-2 virus. (Xiao et al., J Infect, Mar 2020)

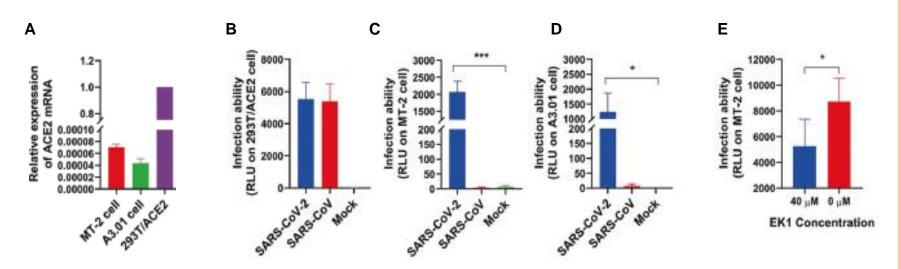
SARS-CoV-2 Immunity: lymphocyte subset counts

Table 1
Demographic and clinical characteristics of 39 patients with COVID-19,

Characteristics (normal range)	Median (IQR) / N (%)	Increased, N (%)	Decreased, N (%)
Age, year	53 (41-61)	-	-
Sex			
Female	20 (51,3)	_	_
Male	19 (48,7)	_	_
Onset to admission, d	5 (3-7)	_	_
Leucocytes $(3.5-9.5 \times 10^9/L)$	4,11 (3,33-5,16)	13 (34,2)	3 (7,9)
Lymphocytes $(1,1-3,2 \times 10^{9}/L)$	0,73 (0,56-1,07)	0	29 (76,3)
T cells (805-4459 × 10 ⁶ /L)	561.0 (300.0-1056.0)	0	24 (61.5)
CD4+ T cells (345-2350 x 106/L)	308,0 (176,0-665,0)	0	22 (56,4)
CD8+ T cells $(345-2350 \times 10^6/L)$	168,0 (117,0-368,0)	0	28 (71,8)
CD4+/CD8+ (0,96-2,05)	1,640 (1,140-2,380)	14 (35,9)	7 (17,9)
B cells (240-1317 × 10 ⁶ /L)	146,0 (56,0-272,0)	0	27 (69,2)
NK cells (210-1514 × 10 ⁶ /L)	136,0 (57,0-207,0)	0	30 (76,9)
Onset to RT-PCR turning negative, d	14 (10-20)	-	- '

Lymphocyte subset counts of all subsets decreased in more than half of the patients on admission. T cells decreased in 24 (61.5%) patients, CD4 + T cells decreased in 22 (56.4%) patients, CD8 + T cells decreased in 28 (71.8%) patients, B cells decreased in 27 (69.2%) patients, and NK cells decreased in 30 (76.9%) patients. Among patients enrolled, the median time of onset to RT-PCR turning negative was 14 days. CD4 + T cell and CD8 + T cell counts were closely related to disease severity and clinical outcome when we compared the counts of lymphocyte subsets in different patient groups. The more serious the disease and the worse the prognosis, the lower were the T cell, CD4 + T cell, and CD8 + T cell counts on admission. Based on these findings, the CD4 + and CD8 + T cell counts in patients with COVID-9 could reflect disease severity and predict disease prognosis and are therefore good biomarkers of SARS-CoV-2 activity. (Liu et al., J. Infect, Apr 2020)

SARS-CoV-2 can infect lymphocytes



A) Expression of ACE2 mRNA in T cells. 293T/ACE2 cells used as a control. B) Infection of pseudotyped SARS-CoV-2 and SARS-CoV on 293T/ACE2 cells. C and D) Infection of pseudotyped T lymphoid cell lines. E) Inhibition of EK1 peptide on pseudotyped SARS-CoV-2 on MT-2 cells. SARS-CoV-2 may infect T-lymphocytes even in the absence of high levels of ACE2. A peptide blocking S-spike/ACE-2 binding (EK1) is able to partially block CoV-2 infectivity at high concentrations, suggesting other mechanisms for viral entry, such as S-protein mediated fusion, or the involvement of other receptors such as CD147 or integrins. However, the virus do not replicate in T-cells. (Wang et al., Cell Mol Immunol, Apr. 2020)



Current Therapies

- 1. Inhibiting the RNA-dependent RNA polymerase: Remdesivir, Faviparavir
- 2. Inhibiting the Viral Protease: Ivermectin, Lopinavir/Ritonavir,
- 3. Blocking Virus-Cell Membrane Fusion: soluble rhACE2, Hydroxychloroquine, Arbidol Hydrochloride (Umifenovir)
- 4. Enhancing the Innate Immune System: anti-cancer NK-based products, Recombinant Interferon
- 5. Attenuating the Inflammatory Response: MSCs, IVIG, SARS-CoV-2-Specific Neutralizing Antibodies, Anti-C5a Monoclonal Antibody, Tocilizumab, Siltuximab, TZLS-501, Sarilumab, Thalidomide, Methylprednisolone, Fingolimod
- 6. Symptomatic control: Bevacizumab

(Tu et al., Int J Mol Sci, Apr 2020)



Top runners vaccines

- 1. mRNA-1273: Moderna's mRNA-1273 is a synthetic strand of mRNA that encodes the prefusion-stabilized viral spike protein
- 2. INO-4800: INO-4800 is a DNA vaccine candidate created by Inovio Pharmaceuticals. INO-4800 is also a genetic vaccine that can be delivered to human cells and translated into proteins to elicit immune responses
- 3. ChAdOx1 nCoV-19: created by the University of Oxford, is composed of a non-replicating adenovirus vector and the genetic sequence of the S protein of SARS-CoV-2
- 4. Stabilized Subunit Vaccines: the University of Queensland is developing a stabilized subunit vaccine based on the molecular clamp technology, which would allow recombinant viral proteins to stably remain in their pre-fusion form
- 5. Nanoparticle-Based Vaccines: Novavax, Inc. is producing a nanoparticle-based vaccine using antigens derived from the coronavirus S protein. The protein is stably expressed in the baculo-virus system, and the product is anticipated to enter phase I trial this summer
- 6. Pathogen-Specific Artificial Antigen-Presenting Cells: genetically modified artificial antigen-presenting cells (aAPCs) that express the conserved domains of the viral structural proteins delivered by lentivirus vector are supposed to evoke the naïve T cells in the human body and lead to dierentiation and proliferation. Trials are now evaluating the safety and immunogenicity of aAPCs alone and in combination with antigen-specific cytotoxic T cells (NCT04299724, NCT04276896).
- 7. Microneedles array based vaccine: the university of Pittsburgh produced subunit vaccines fused with a foldon trimerization domain to mimic the native viral structure. In variant constructs, immune stimulants (RS09 or flagellin, as TLR4 or TLR5 agonists, respectively) were engineered into this trimeric design.

(Tu et al., Int J Mol Sci, Apr 2020; Kim et al., Ebiomedicine, Apr 2020)



Unsolved questions

- > Role of accessory genes
- > Transcriptional mechanisms are not fully clear
- > Unusual splicing events
- > RNA Epimodifications
- > Addressing the fidelity of RdRp upon newly occurred mutations
- > Addressing the role of RdRp 14408 containing region
- > Molecular mechanism of cell entry
- >....?



References

- 1. Tu YF, et al. A Review of SARS-CoV-2 and the Ongoing Clinical Trials. Int J Mol Sci. 2020 Apr 10;21(7). pii: E2657. doi: 10.3390/iims21072657.
- 2. Zhou F, Yu T, Du R, Fan G, Liu Y, Liu Z, Xiang J, Wang Y, Song B, Gu X, Guan L, Wei Y, Li H, Wu X, Xu J, Tu S, Zhang Y, Chen H, Cao B. Clinical course and risk factors for mortality of adult inpatients with COVID-19 in Wuhan, China: a retrospective cohort study. Lancet. 2020 Mar 28;395(10229):1054-1062. doi: 10.1016/S0140-6736(20)30566-3.
- 3. Wölfel R, Corman VM, Guggemos W, Seilmaier M, Zange S, Müller MA, Niemeyer D, Jones TC, Vollmar P, Rothe C, Hoelscher M, Bleicker T, Brünink S, Schneider J, Ehmann R, Zwirglmaier K, Drosten C, Wendtner C. Virological assessment of hospitalized patients with COVID-2019. Nature. 2020 Apr 1. doi: 10.1038/s41586-020-2196-x.
- 4. Yuan M, Wu NC, Zhu X, Lee CD, So RTY, Lv H, Mok CKP, Wilson IA. A highly conserved cryptic epitope in the receptor-binding domains of SARS-CoV-2 and SARS-CoV. Science. 2020 Apr 3. pii: eabb7269. doi: 10.1126/science.abb7269.
- 5. Sigrist CJ, Bridge A, Le Mercier P. A potential role for integrins in host cell entry by SARS-CoV-2 Antiviral Res. 2020 May;177:104759. doi: 10.1016/j.antiviral.2020.104759.
- 6. Ou X, Liu Y, Lei X, Li P, Mi D, Ren L, Guo L, Guo R, Chen T, Hu J, Xiang Z, Mu Z, Chen X, Chen J, Hu K, Jin Q, Wang J, Qian Z. Characterization of spike glycoprotein of SARS-CoV-2 on virus entry and its immune cross-reactivity with SARS-CoV Nat Commun. 2020 Mar 27;11(1):1620. doi: 10.1038/s41467-020-15562-9.
- 7. Wrapp D, Wang N, Corbett KS, Goldsmith JA, Hsieh CL, Abiona O, Graham BS, McLellan JS. Cryo-EM structure of the 2019-nCoV spike in the prefusion conformation. Science. 2020 Mar 13;367(6483):1260-1263. doi: 10.1126/Science.abb2507
- 8. Guzzi PH, Mercatelli D, Ceraolo C, Giorgi FM. Master Regulator Analysis of the SARS-CoV-2/Human Interactome. J Clin Med. 2020 Apr 1;9(4). pii: E982. doi: 10.3390/jcm9040982.

CoVid

Day 21/04/20

9. Srinivasan S, Cui H, Gao Z, Liu M, Lu S, Mkandawire W, Narykov O, Sun M, Korkin D. Structural Genomics of SARS-CoV-2 Indicates Evolutionary Conserved Functional Regions of Viral Proteins. Viruses. 2020 Mar 25;12(4) pii: E360. doi: 10.3390/v12040360.

- 10. Tresoldi I, Sangiuolo CF, Manzari V, Modesti A. SARS-COV-2 and infectivity: Possible increase in infectivity associated to integrin motif expression. J Med Virol. 2020 Apr 4. doi: 10.1002/jmv.25831
- 11. Hoffmann M, Kleine-Weber H, Schroeder S, Krüger N, Herrler T, Erichsen S, Schiergens TS, Herrler G, Wu NH, Nitsche A, Müller MA, Drosten C, Pöhlmann S. SARS-CoV-2 Cell Entry Depends on ACE2 and TMPRSS2 and Is Blocked by a Clinically Proven Protease Inhibitor Cell. 2020 Apr 16;181(2):271-280.e8. doi: 10.1016/j.cell.2020.02.052.
- 12. Lukassen S, Chua RL, Trefzer T, Kahn NC, Schneider MA, Muley T, Winter H, Meister M, Veith C, Boots AW, Hennig BP, Kreuter M, Conrad C, Eils R. SARS-CoV-2 receptor ACE2 and TMPRSS2 are primarily expressed in bronchial transient secretory cells EMBO J. 2020 Apr 14:e105114. doi: 10.15252/embj.2020105114.
- 13. Wang Q, Zhang Y, Wu L, Niu S, Song C, Zhang Z, Lu G, Qiao C, Hu Y, Yuen KY, Wang Q, Zhou H, Yan J, Qi J. Structural and Functional Basis of SARS-CoV-2 Entry by Using Human ACE2 Cell. 2020 Apr 7. pii: S0092-8674 (20)30338-X. doi: 10.1016/j.cell.2020.03.045.
- 14. Zhou P, Yang XL, Wang XG, Hu B, Zhang L, Zhang W, Si HR, Zhu Y, Li B, Huang CL, Chen HD, Chen J, Luo Y, Guo H, Jiang RD, Liu MQ, Chen Y, Shen XR, Wang X, Zheng XS, Zhao K, Chen QJ, Deng F, Liu LL, Yan B, Zhan FX, Wang YY, Xiao GF, Shi ZL. A pneumonia outbreak associated with a new coronavirus of probable bat origin Nature. 2020 Mar;579(7798):270-273. doi: 10.1038/s41586-020-2012-7.
- 15. Kim D, Lee J-Y, Yang J-S, Kim JW, Kim VN, Chang H. The architecture of SARS-CoV-2 transcriptome. Cell, 2020 Apr 18. pii: \$0092-8674(20)30406-2. doi: 10.1016/j.cell.2020.04.011.
- 16. Pachetti M, Marina B, Benedetti F, Giudici F, Mauro E, Storici P, Masciovecchio C, Angeltti S, Ciccozzi M, Gallo RC, Zella D, Ippodrino R. Emerging SARS-CoV-2 mutation hot spots include a novel RNA-dependent-RNA polymerase variant. J Transl Med, in press.
- 17. Zhang T, Wu Q, Zhang Z. Probable Pangolin Origin of SARS-CoV-2 Associated with the COVID-19 Outbreak. Curr Biol. 2020 Apr 6;30(7):1346-1351.e2. doi: 10.1016/j.cub.2020.03.022.

CoVid

Day 21/04/20

18. Forster P, Forster L, Renfrew C, Forster M. Phylogenetic network analysis of SARS-CoV-2 genomes. Proc Natl Acad Sci U S A. 2020 Apr 8. pii: 202004999.doi: 10.1073/pnas.2004999117.

- 19. Zhao J, Yuan Q, Wang H, Liu W, Liao X, Su Y, Wang X, Yuan J, Li T, Li J, Qian S, Hong C, Wang F, Liu Y, Wang Z, He Q, Li Z, He B, Zhang T, Fu Y, Ge S, Liu L, Zhang J, Xia N, Zhang Z. Antibody responses to SARS-CoV-2 in patients of novel coronavirus disease 2019. Clin Infect Dis. 2020 Mar 28. pii: ciaa344. doi10.1093/cid/ciaa344.
- 20. Du Z, Zhu F, Guo F, Yang B, Wang T. Detection of antibodies against SARS-CoV-2 in patients with COVID-19 J Med Virol. 2020 Apr 3. doi: 10.1002/jmv.25820.
- 21. Liu Z, Long W, Tu M, Chen S, Huang Y, Wang S, Zhou W, Chen D, Zhou L, Wang M, Wu M, Huang Q, Xu H, Zeng W, Guo L. Lymphocyte subset (CD4 + , CD8 +) counts reflect the severity of infection and predict the clinical outcomes in patients with COVID-19. J Infect. 2020 Apr 10. pii: S0163-4453(20)30182-1. doi: 10.1016/j.jinf.2020.03.054.
- Mar 21. pii: S0163-4453(20)30138-9. doi: 10.1016/j.jinf.2020.03.012.

 23. Wang X, Xu W, Hu G, Xia S, Sun Z, Liu Z, Xie Y, Zhang R, Jiang S, Lu L. SARS-CoV-2 infects T lymphocytes

through its spike protein-mediated membrane fusion Cell Mol Immunol. 2020 Apr 7. doi: 10.1038/s41423-020-

22. Xiao DAT, Gao DC, Zhang DS. Profile of Specific Antibodies to SARS-CoV-2: The First Report. J Infect. 2020

0424-9.

24. Conti P, Younes A. Coronavirus COV-19/SARS-CoV-2 Affects Women Less Than Men: Clinical Response to

Viral Infection. J Biol Regul Homeost Agents. 2020 Apr 7;34(2). doi: 10.23812

- 25. Stopsack KH, Mucci LA, Antonarakis ES, Nelson PS, Kantoff PW. TMPRSS2 and COVID-19: Serendipity or opportunity for intervention? Cancer Discov. 2020 Apr 10. pii: CD-20-0451. doi: 10.1158/2159-8290.CD-20-0451.
- 26. Kim E, Erdos G, Huang S, Kenniston TW, Balmert SC, Carey CD, Raj VS, Epperly MW, Klimstra WB, Haagmans BL, Korkmaz E, Falo LD Jr, Gambotto A. Microneedle array delivered recombinant coronavirus vaccines Immunogenicity and rapid translational development. EBioMedicine. 2020 Apr 1:102743. doi:10.1016/j.ebiom.2020.102743.
- 27. Uhler C, Shivashankar GV. Mechano-genomic regulation of coronaviruses and its interplay with ageing.

 Nat Rev Mol Cell Biol. 2020 Apr 2. doi: 10.1038/s41580-020-0242-z.
- 28. Coutard B, Valleb C, de Lamballerie X, Canard B, Seidahc NG, Decrolyb E. The spike glycoprotein of the new coronavirus 2019-nCoV contains a furin-like cleavage site absent in CoV of the same clade. Antiviral Res, 2020 Apr;176:104742. doi: 10.1016/j.antiviral.2020.104742.